

19. Modeling of facade elements with switchable U-value / Pflug T., Nestle N., Kuhn T. E., Siroux M., Maurer C. // Energy and Buildings. 2018. Vol. 164. P. 1–13. doi: 10.1016/j.enbuild.2017.12.044
20. Investigations on Physical-mechanical Properties of Effective Thermal Insulation Materials from Fibrous Hemp / Kremensas A., Stapulionienė R., Vaitkus S., Kairytė A. // Procedia Engineering. 2017. Vol. 172. P. 586–594. doi: 10.1016/j.proeng.2017.02.069
21. Energy performance of a ventilated façade by simulation with experimental validation / Aparicio-Fernández C., Vivancos J.-L., Ferrer-Gisbert P., Royo-Pastor R. // Applied Thermal Engineering. 2014. Vol. 66, Issue 1-2. P. 563–570. doi: 10.1016/j.applthermaleng.2014.02.041
22. Kolosov A. E. Efficiency of Liquid Reactoplastic Composite Heterofrequency Ultrasonic Treatment // Chemical and Petroleum Engineering. 2014. Vol. 50, Issue 3-4. P. 268–272. doi: 10.1007/s10556-014-9893-y
23. Review on ultrasonic fabrication of polymer micro devices / Sackmann J., Burlage K., Gerhardy C., Memering B., Liao S., Schomburg W. K. // Ultrasonics. 2015. Vol. 56. P. 189–200. doi: 10.1016/j.ultras.2014.08.007
24. Procedure for analysis of ultrasonic cavitator with radiative plate / Kolosov A. E., Sivetskii V. I., Kolosova E. P., Lugovskaya E. A. // Chemical and Petroleum Engineering. 2013. Vol. 48, Issue 11-12. P. 662–672. doi: 10.1007/s10556-013-9677-9
25. Yeromin A. V. Systema kompleksnoi termomodernizatsiyi budivel i sporud za Yerominym: Pat. No. 115858 C2 UA. MPK F24D3/00, F16L59/00. No. a201709331; declared: 25.09.2017; published: 26.12.2017, Bul. No. 24.
26. Yeromin A. V. Sposib kompleksnoi termomodernizatsiyi budivel i sporud za Yerominym: Pat. No. 115760 C2 UA. MPK F24D3/00, F16L59/00. No. a201709333; declared: 25.09.2017, published: 11.11.2017, Bul. No. 23.

*Запропоновано метод формування температурних режимів мікроклімату в тваринницьких спорудах різного функціонального призначення з застосуванням багатошарової грійоючої підлоги. Розроблено структурну математичну модель, що дозволяє при заданому режимі роботи т-ярусних трубчастих нагрівачів з урахуванням теплопровідності кожного шару теплогенеруючих модулів визначити конструктивно-теплотехнічні параметри. Це дає можливість забезпечувати формування оптимального температурного поля на поверхні багатошарової структури грійоючої підлоги*

*Ключові слова: температурні поля, грійоюча підлога, теплогенеруючі модулі, трубчасті нагрівачі, шарувата структура*

*Предложен метод формирования температурных режимов микроклимата в животноводческих сооружениях различного функционального назначения с применением многоуровневого греющего пола. Разработана структурная математическая модель, которая позволяет в зависимости от режима работы т-ярусных трубчатых нагревателей с учетом теплопроводности каждого уровня теплогенерирующих модулей определять конструктивно-теплотехнические параметры. Это позволяет обеспечивать формирование оптимального температурного поля на поверхности многоуровневой структуры греющего пола*

*Ключевые слова: температурные поля, греющий пол, теплогенерирующие модули, трубчатые нагреватели, слоистая структура*

UDC 631.2:631.171:65.011.56

DOI: 10.15587/1729-4061.2018.121827

## EFFECT OF THERMAL FIELD DISTRIBUTION IN THE LAYERED STRUCTURE OF A HEATING FLOOR ON THE TEMPERATURE OF ITS SURFACE

**M. Romanchenko**  
PhD\*

E-mail: betso@ukr.net

**A. Slesarenko**

Doctor of Physical and Mathematical Sciences,  
Professor, Pensioner

**M. Kundenko**

Doctor of Technical Sciences, Professor\*

E-mail: betso@ukr.net

\*Department of integrated  
electrotechnologies and processes  
Educational-scientific institute of power engineering  
and computer technologies  
Kharkiv Petro Vasylenko National Technical  
University of Agriculture  
Rizdviana str., 19, Kharkiv, Ukraine, 61012

### 1. Introduction

Food security of the country and the well-being of people are largely determined by the performance efficiency of agriculture, including livestock industry. High quality,

competitive livestock products, including pork, cannot be obtained without the development and implementation of modern resource-efficient technologies based on automated electrotechnical complexes. The functionality of the systems of these complexes must fully ensure veterinary-sanitary re-

quirements put forward to the conditions of keeping animals during production cycle. In this case, scientifically substantiated parameters and operation modes of power electrical equipment make it possible not only to reduce the cost of pork production, but also contribute to the improvement of production culture in the industry. In addition, devising a resource-efficient electrotechnology reduces the negative impact of industrial waste on the environment and provides for broader involvement of untraditional and renewable sources of energy (URSE) [1].

Special attention is paid to the systems designed to create temperature regimes of the microclimate of premises where animals of different age groups are kept. There is a need to provide premises with the heat modes that are almost twice different (for sows – 18–20 °C, for piglets during first day of birth – 38–39 °C). This is one of the reasons why energy expenditures account for almost 60 % of pork production cost [2, 3].

All the above testifies to the importance of this issue in terms of developments aimed at improving the existing, and creating the new, more energy- and resource-efficient means to create optimum microclimatic modes. This would make it possible to increase the volume of production of high-quality agricultural products.

---

## 2. Literature review and problem statement

---

An analysis of data from the scientific-technical literature that addresses technologies and means for creating the microclimate in livestock production facilities (PF) revealed several operational and structural drawbacks [4, 5]. This includes known “classic” systems that operate according to a “top-down” principle and require fundamental improvement [6, 7]. A confirmation of the objectivity of a given hypothesis, specifically regarding the low efficiency of energy use, can be a relative indicator of specific energy consumption, which, as compared with similar indicators in the industrially developed countries, is larger by 2.5–3 times.

In this case, we compare energy costs that enable technological processes of pork production in countries located in the same geographic-climatic zone (48–50° North latitude) [8].

Leading experts on the development of advanced energy-saving systems of microclimate for PF consider one of the effective directions to be the development of energy-saving electrotechnical complexes. The structure of these complexes must include at least electro-heat accumulation modules that power heaters using traditional and URSE. A fundamental difference of such systems is that they can work in line with the “bottom-up” principle [9]. These systems, in addition to improving the efficiency of energy use and feed stock, can operate under autonomous mode of heating PF utilizing existing potential capacity of traditional and non-traditional renewable sources of energy (URSE). In addition, enabling an optimal thermal mode of the surface of heating floor in technologically active zones (TAZ) at PF makes it possible to maximally accumulate “excessive” electricity from different sources. This is especially true of energy consumption during downtime in daily load at these farms, taking into consideration the possibility to pay for the consumed off-peak electricity according to multi-zone preferential tariffs [10].

We have chosen, as a proposed variant of the multilevel electro-heat accumulation heating system (MEHHS) whose

heat-generating modules are examined, a structural design with 3 tiers of active heating units (layers of the heat generating module). The use of such an assembly of MEHHS is predetermined by the necessity to rationally solve functionally important tasks. These include improving the technological reliability of electrotechnical complex and creation of conditions to ensure the process of flexible and prompt generation of thermal modes of the microclimate at PF. At the same time, researchers of electro-heat accumulation systems of microclimate with heating floors chose to solve direct problems of thermal conductivity in order to determine electric power and heat engineering characteristics, modes of operation, geometrical parameters of heat-generating modules [11, 12]. Using the method of sequential approximation, they investigated variants with a different set of ratios, geometrical parameters and energy components, which are supplied to the electric heaters of these structures. Such an approach makes it difficult, or fundamentally impossible, to solve the tasks on strict compliance with optimal temperature modes under condition of rational and efficient use of energy resources of traditional and URSE. To some extent, this is explained by the fact that it is impossible to introduce to the algorithm and, accordingly, to the program for solving direct problems of thermal conductivity, discrete information that reflects the preset standards on heating the floor surface in TAZ at PF [13].

A fundamentally different approach to resolving a given task implies stating and solving respective inverse problems of thermal conductivity in order to determine the energy components that are supplied to the m-tiered units of special tubular electric heaters (STH) in heat-generating modules. Only those programs and algorithms that are built using the inverse problems of thermal conductivity allow introducing to their statement the specified temperature modes for heating the floor surface as the data of a thermophysical experiment. In addition, the inverse problems of thermal conductivity make it possible to enable control over supply of respective energy components to STH of MEHHS taking into consideration meteorological conditions that affect the microclimate of production facility [14].

---

## 3. The aim and objectives of the study

---

The aim of present work is to conduct a theoretical study into the influence of thermal field distribution of the layered structure of heating floor on the temperature of its surface.

To accomplish the aim, the following tasks have been set:

- to determine the distribution of a steady temperature field in the layered structure of MEHHS in the form of a prism;
- to devise a mathematical model of the heating system of MEHHS with respect to the thermal conductivity of the layered structure of heat-generating modules.

---

## 4. Materials and research methods

---

The presence of MEHHS in the circuit of an automated electrotechnical complex makes it possible to form optimum temperature modes of the microclimate by the heating floor in livestock facilities of different functional purpose. Functionally, MEHHS (Fig. 1) is one kind of systems for autonomous distributed electric heating, in which electrical

energy is converted into thermal energy in STH, combined in the m-tiered units of heat-generating modules, located in the heat accumulation filler of the trench dug in soil of the floor of TAZ at PF.

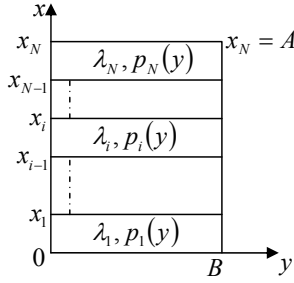


Fig. 1. Cross-section of MEHHS model

These systems, when using structural-functional control over energy fluxes of power to the heaters of STH in MEHHS, make it possible to solve several functional and operational tasks. These include ensuring the optimum value of temperature at the floor surface and at the preset height in TAZ, maximal energy saving and optimal electro heat accumulation, providing quality support to technological processes for manufacturing livestock products [12].

Physical model of the multilayer structure of heat generating module in MEHHS is considered in the form of a rectangular prism whose top is the floor surface while the entire body of the heating structure is submerged in the soil.

Solving the boundary value problem of thermal conductivity relates to the function of steady temperature distribution inside the prism (thermal field), restricted by flat boundary surfaces of a rectangular shape. The rectangular prism is structured inside – it consists of  $N$  homogeneous flat layers that border each other in the region of adjacent borders; in this case, we accept that the thermal contact between layers is imperfect (we have the finite thermal resistance).

The desired steady thermal field in the middle of the layered structure  $t = t(x, y, z)$  consists of  $N$  interdependent temperature fields

$$u_i = u_i(x, y, z), \quad (1)$$

which are implemented (established) within the  $i$ -th homogeneous layer.

Functions (1) that are searched for in regions  $x_{i-1} \leq x \leq x_i$ ,  $0 \leq y \leq B$ ,  $0 \leq z \leq C$  ( $i=1, 2, \dots, N$ ) satisfy the equation of thermal conductivity in the form:

$$\frac{\partial^2 u_i}{\partial x^2} + \frac{\partial^2 u_i}{\partial y^2} + \frac{\partial^2 u_i}{\partial z^2} = -\frac{1}{\lambda_i} p_i(y) q_i(z), \quad (2)$$

where  $\lambda_i$  is the coefficient of thermal conductivity of the  $i$ -th layer of heating structure of MEHHS,  $\text{W}\cdot\text{m}^{-1}\cdot\text{K}^{-1}$ ;  $p_i(y)$  is the power density of heat sources of STH distributed in MEHHS,  $\text{W}/\text{m}^3$ ;  $q_i(z)$  is the weight function of step type, which describes differential heating of the floor surface in separate areas of TAZ along the heating unit.

Their levels are selected in the range of values of 0.5–2 relative to a certain mean temperature to fulfil technological tasks on creating a microclimate in the room along one separate line of the floor.

Solution to equation (2) with a set of focused sources in each of the layers  $i=1, 2, \dots, N$  will be found using a method of finite integral transforms (FIT). Thermal field in each of the layers will be searched for in the form of 2 components (according to the principle of superposition):

$$u_i(x, y, z) = t_{0i} + v_{0i}(x, y, z) + v_i(x, y, z), \quad (3)$$

where function

$$\tilde{v}_{0i}(x, y, z) = t_{0i} + v_{0i}(x, y, z) \quad (4)$$

is the solution to the Laplace homogeneous equation  $\Delta \tilde{v}_{0i} = 0$ , and function  $v_i(x, y, z)$  is the partial solution to the original inhomogeneous equation with homogeneous boundary conditions.

Next, we give separately the problems of thermal conductivity relative to functions  $v_i(x, y, z)$  and  $\tilde{v}_i(x, y, z)$  with corresponding boundary conditions:

$$\frac{\partial^2 v_{0i}}{\partial x^2} + \frac{\partial^2 v_{0i}}{\partial y^2} + \frac{\partial^2 v_{0i}}{\partial z^2} = 0, \quad (5)$$

$$v_{0i}|_{x=0} = t_0 - t_{0i}, \quad (6)$$

$$-\lambda_N \frac{\partial u_{0N}}{\partial x} \Big|_{x=x_N} = \alpha [v_{0N}|_{x_N} - (t_c - t_{0N})], \quad (7)$$

$$\frac{\partial u_{0i}}{\partial y} \Big|_{y=0} = 0, \quad (8)$$

$$\left( v_{0i} + h_y \frac{\partial v_{0i}}{\partial y} \right) \Big|_{y=B} = 0, \quad (9)$$

$$\frac{\partial u_{0i}}{\partial z} \Big|_{z=0} = 0, \quad (10)$$

$$\left( v_{0i} + h_z \frac{\partial v_{0i}}{\partial z} \right) \Big|_{z=C} = 0, \quad (11)$$

$$\frac{\partial^2 v_{0i}}{\partial x^2} + \frac{\partial^2 v_{0i}}{\partial y^2} + \frac{\partial^2 v_{0i}}{\partial z^2} = -\frac{1}{\lambda_i} p_i(y) q_i(z), \quad (12)$$

$$v_i|_{x=0} = 0, \quad (13)$$

$$-\lambda_N \frac{\partial u_N}{\partial x} \Big|_{x=x_N} = \alpha v_N|_{x_N}, \quad (14)$$

$$\frac{\partial u_i}{\partial y} \Big|_{y=0} = 0, \quad (15)$$

$$\left( v_i + h_y \frac{\partial v_i}{\partial y} \right) \Big|_{y=B} = 0, \quad (16)$$

$$\frac{\partial u_i}{\partial z} \Big|_{z=0} = 0, \quad (17)$$

$$\left( v_{0i} + h_z \frac{\partial v_{0i}}{\partial z} \right) \Big|_{z=C} = 0. \quad (18)$$

The constructed (full) solution (3) satisfies original equation (2) with boundary conditions on the outer boundary flat surfaces. In addition, solutions obtained to each of the layers  $i=1, 2, \dots, N$  should be aligned at the borders of flat layers  $x=x_i (i=1, 2, \dots, N-1)$  for temperatures and heat fluxes at the borders; in this case, separately for each set of functions, that is, for sets  $v_{0i}(x, y, z)$  and  $v_i(x, y, z), i=1, 2, \dots, N$ .

Using a standard procedure for solving such problems applying a method of finite integral transforms (FIT), we shall exclude, consequentially, differential operations along the  $z$  axis and the  $y$  axis.

The kernel of transform  $K(z, v)$ , which excludes the operation of differentiation along the  $z$  axis, is the solution to the boundary value problem for region  $0 \leq z \leq L (L=C)$ :

$$\frac{\partial^2 K}{\partial z^2} + v^2 K = 0; \tag{19}$$

$$\left. \frac{\partial K}{\partial z} \right|_{z=0} = 0; \left( K + h \frac{\partial K}{\partial z} \right) \Big|_{z=L} = 0. \tag{20}$$

The stated problem is the Sturm-Liouville problem on determining the eigenvalues, the solution to which is the function  $\cos(vz)$ , which automatically satisfies condition 1 (20), and which, in addition, must satisfy condition 2 (20):

$$(\cos(vz) - hv \sin(vz)) \Big|_{z=L} = 0; \text{ctg}(vL) = hv. \tag{21}$$

The number of eigenvalues, defined from (21), makes it possible to construct a system of eigenfunctions.

$$K_p(z) \equiv K_p(v_p z) = \cos(v_p z). \tag{22}$$

We shall employ a given FIT to equation (5) with respect to the introduction of FIT of the original coordinate function  $v_{0i}(x, y, z)$ :

$$\bar{v}_{0i}^p(x, y, v_p) = \frac{1}{L} \int_0^L K(v_p z) \cdot v_{0i}(x, y, z) dz;$$

$$\frac{1}{L} \int_0^L K(z) \dots dz$$

$$\frac{\partial^2 v_{0i}}{\partial x^2} + \frac{\partial^2 v_{0i}}{\partial y^2} + \frac{\partial^2 v_{0i}}{\partial z^2} = 0;$$

$$\frac{\partial^2 \bar{v}_{0i}}{\partial x^2} + \frac{\partial^2 \bar{v}_{0i}}{\partial y^2} + \frac{1}{L} \int_0^L K_p(z) \frac{\partial^2 v_{0i}}{\partial z^2} dz = 0;$$

$$\frac{1}{L} \int_0^L K_p(z) \frac{\partial^2 v_{0i}}{\partial z^2} dz = \frac{1}{L} K_p \frac{\partial v_{0i}}{\partial z} \Big|_0^L - \frac{1}{L} \int_0^L K_p'(z) \frac{\partial v_{0i}}{\partial z} dz =$$

$$= \frac{1}{L} K_p \frac{\partial v_{0i}}{\partial z} \Big|_0^L - \frac{1}{L} K_p v_{0i} \Big|_0^L + \frac{1}{L} \int_0^L K_p''(z) v_{0i}(z) dz =$$

$$= \frac{1}{L} \left( K_p \frac{\partial v_{0i}}{\partial z} - \frac{\partial K_p}{\partial z} v_{0i} \right) \Big|_0^L - v_p^2 \bar{v}_{0i}(x, y, v_p).$$

Using boundary conditions makes it possible to obtain a sequence of equations related to each layer of the structure under consideration

$$\frac{\partial^2 \bar{v}_{0i}^p}{\partial x^2} + \frac{\partial^2 \bar{v}_{0i}^p}{\partial y^2} - v_p^2 \bar{v}_{0i}^p(x, y, v_p) = 0, \quad p = 1, 2, \dots \tag{23}$$

Applying the found FIT  $\bar{v}_{0i}(x, y, v_p)$ , restoration of the original function is performed using formula:

$$v_{0i}(x, y, z) = \sum_{p=1}^P \frac{\cos(v_p z)}{N_p} \bar{v}_{0i}^p(x, y, v_p), \tag{24}$$

where

$$N_p = \frac{1}{L} \int_0^L \cos^2(v_p z) dz = \frac{1}{2} \left[ 1 + \frac{\left(\frac{h}{L}\right)}{1 + (v_p h)^2} \right]. \tag{25}$$

Equation (23), obtained by applying FIT with kernel  $K_p(z)$  to the original equation, is solved relative to the new functions that should satisfy conditions (26)–(29):

$$\bar{v}_{0i}^p(x, y, v_p) \Big|_{x=0} = (t_0 - T_{\text{bound.1}}) \sin c(v_p L); \tag{26}$$

$$\left( \bar{v}_{0N}^p + \frac{\lambda_N}{\alpha} \cdot \frac{\partial \bar{v}_{0N}^p}{\partial x} \right) \Big|_{x=x_N} = (t_c - T_{\text{bound.N}}) \sin c(v_p L); \tag{27}$$

$$\frac{\partial \bar{v}_{0i}^p}{\partial y} \Big|_{y=0} = 0; \tag{28}$$

$$\left( \bar{v}_{0i}^p + h \frac{\partial \bar{v}_{0i}^p}{\partial y} \right) \Big|_{y=B} = 0. \tag{29}$$

$$\frac{1}{L} \int_0^L \cos v_p z dz = \frac{1}{v_p L} \sin v_p z \Big|_0^L = \frac{\sin v_p L}{v_p L} = \sin c(v_p L),$$

$$\begin{aligned} N_p &= \frac{1}{2L} \int_0^L (1 + \cos 2v_p z) dz = \\ &= \frac{1}{2} + \frac{1}{2L} \int_0^L \cos 2v_p z dz = \frac{1}{2} + \frac{1}{4v_p L} \sin(2v_p L) = \\ &= \frac{1}{2} + \frac{1}{2} \sin v_p L \frac{\cos v_p L}{v_p L} = \frac{1}{2} \left[ 1 + \frac{\left(\frac{h}{L}\right)}{1 + (hv_p)^2} \right], \end{aligned}$$

$$\text{ctg} v_p L = hv_p; \quad \cos v_p L = hv_p \sin v_p L.$$

The kernel of FIT  $K(y, \mu)$ , which excludes differentiation along  $y$ , is the solution to the boundary value problem for region  $0 \leq y \leq B$ :

$$\frac{\partial^2 K(y, \mu)}{\partial y^2} + \mu^2 K(y, \mu) = 0; \tag{30}$$

$$\frac{\partial K}{\partial y} \Big|_{y=0} = 0; \left( K + h \frac{\partial K}{\partial y} \right) \Big|_{y=B} = 0. \tag{31}$$

Solution to (30) with respect to the first condition from (31) is the function  $\cos(\mu y)$ , which should be subjected to the second condition from (31), that is:

$$\text{ctg}(\mu B) = h\mu. \tag{32}$$

This equation gives rise to a number of eigenvalues  $\mu_q^2$  and, accordingly, a set of eigenfunctions:

$$K_q(y) \equiv K_q(\mu_q y) = \cos(\mu_q y), \quad q = 1, 2, \dots \quad (33)$$

We shall introduce FIT of functions and  $\bar{v}_{0i}(x, y, y_p)$  along the  $y$  coordinate in the form:

$$\bar{v}_{0i}^{p,q}(x; \mu_q; v_p) = \frac{1}{B} \int_0^B K_q(\mu_q y) \bar{v}_{0i}^p(x, y, v_p) dy, \quad (34)$$

$$\frac{1}{B} \int_0^B K_q(y) \dots dy; \quad \frac{\partial^2 \bar{v}_{0i}^{p,q}}{\partial x^2} + \frac{\partial^2 \bar{v}_{0i}^{p,q}}{\partial y^2} - v_p \bar{v}_{0i}^{p,q} = 0.$$

Similar to the steps performed above, it is possible to obtain:

$$\begin{aligned} & \frac{\partial^2 \bar{v}_{0i}^{p,q}}{\partial x^2} - v_p \bar{v}_{0i}^{p,q} + \frac{1}{B} \int_0^B K_q(y) \frac{\partial^2 \bar{v}_{0i}^{p,q}}{\partial y^2} dy = 0; \\ & \frac{1}{B} \int_0^B K_q(y) \frac{\partial^2 \bar{v}_{0i}^{p,q}}{\partial y^2} dy = \frac{1}{B} K_q \frac{\partial \bar{v}_{0i}^p}{\partial y} \Big|_0^B - \frac{1}{B} \int_0^B K_q' \frac{\partial \bar{v}_{0i}^p}{\partial y} dy = \\ & = \frac{1}{B} \left( K_q \frac{\partial \bar{v}_{0i}^p}{\partial y} - \frac{\partial K_q}{\partial y} \bar{v}_{0i}^p \right) \Big|_0^B + \frac{1}{B} \int_0^B K_q' \bar{v}_{0i}^p dy = \\ & \frac{1}{B} \left( K_q \frac{\partial \bar{v}_{0i}^p}{\partial y} - \frac{\partial K_q}{\partial y} \bar{v}_{0i}^p \right) \Big|_{y=B} - \mu_q^2 \bar{v}_{0i}^{p,q} = -\mu_q^2 \bar{v}_{0i}^{p,q}, \end{aligned}$$

$\left( K_q \frac{\partial \bar{v}_{0i}^p}{\partial y} - \frac{\partial K_q}{\partial y} \bar{v}_{0i}^p \right)$  – parenthesis at  $y=0$  is “reset to zero” given (28), (31), the second term transforms with respect to equation (30):

$$\frac{\partial \bar{v}_{0i}^p}{\partial y} \Big|_{y=B} = -\frac{\bar{v}_{0i}^p}{h}; \quad \frac{\partial K_q}{\partial y} \Big|_{y=B} = -\frac{K_q}{h}.$$

Upon two successively performed FIT, the original Laplace differential equation takes the form:

$$\frac{\partial^2 \bar{v}_{0i}^{p,q}}{\partial x^2} - (v_p^2 + \mu_q^2) \bar{v}_{0i}^{p,q} = 0; \quad p, q = 1, 2, \dots \quad (35)$$

In line with transform (34), functions must satisfy the following boundary conditions:

$$\begin{aligned} & \bar{v}_{0i}^{p,q}(x; \mu_q; v_p) \Big|_{x=0} = \\ & = (t_0 - T_{p1}) \sin c(v_p L) \sin c(\mu_q B); \end{aligned} \quad (36)$$

$$\begin{aligned} & \left( \bar{v}_{0N}^{p,q} + \frac{\lambda_N}{\alpha} \frac{\partial \bar{v}_{0N}^{p,q}}{\partial x} \right) \Big|_{t=x_N} = \\ & = (t_{epN} T) \sin c(v L) \sin c(\mu B). \end{aligned} \quad (37)$$

Given the results with respect to conditions (26), (27), as well as the conditions for aligning the sets of functions (36), we restore the originals of functions:

$$\bar{v}_{0i}^p(x, y, v_p) = \sum_{q=1}^Q \frac{\cos(\mu_q y)}{N_q} \cdot \bar{v}_{0i}^{p,q}(x; \mu_q; v_p), \quad (38)$$

where

$$N_q = \frac{1}{B} \int_0^B \cos^2(\mu_q y) dy = \frac{1}{2} \left[ 1 + \frac{\left(\frac{h}{B}\right)^2}{1 + (\mu_q h)^2} \right]. \quad (39)$$

Considering (29), (30), a general expression for the desired coordinate functions  $v_{0i}(x, y, z)$ , through their FIT representations, can be written in the form:

$$\begin{aligned} & v_{0i}(x, y, z) = \\ & = 4 \sum_{p=1}^P \frac{\cos(v_p z)}{\left[ 1 + \frac{(h/L)^2}{1 + (hv_p)^2} \right]} \cdot \sum_{q=1}^Q \frac{\cos(\mu_q y)}{\left[ 1 + \frac{(h/B)^2}{1 + (hv_p)^2} \right]} \cdot \bar{v}_{0i}^{p,q}(x; \mu_q; v_p). \end{aligned} \quad (40)$$

Similarly built is the solution to functions  $v_i(x, y, z)$ , which are determined by the distribution of heat sources in the heating structure (HS) of MEHHS. It can be written in the form of a double row for the eigenfunctions of respective Sturm-Liouville problems:

$$\begin{aligned} & v_i(x, y, z) = \\ & = 4 \sum_{p=1}^P \frac{\cos(v_p z)}{\left[ 1 + \frac{(h/L)^2}{1 + (hv_p)^2} \right]} \cdot \sum_{q=1}^Q \frac{\cos(\mu_q y)}{\left[ 1 + \frac{(h/B)^2}{1 + (hv_p)^2} \right]} \cdot \bar{v}_i^{p,q}(x; \mu_q; v_p). \end{aligned} \quad (41)$$

Functions (34) and (36) are determined by a combination of functions of hyperbolic sine and cosine from argument  $(v_p^2 + \mu_q^2)(x \cdot x)$  with undefined coefficients. The latter are derived from the solution to the systems of  $2N$  inhomogeneous linear equations. It should be noted that functions  $v_{0i}(x, y, z)$  are determined by the ambient temperature ( $t, t_c, T_{\Gamma p, i}$ ) and comply with the Laplace equation at zero sources of HS ( $p_i = 0$ ); functions  $v_i(x, y, z)$  are determined by the distribution of sources  $p_i(y, z)$  in HS at zero (homogeneous) boundary conditions at HS borders and satisfy alignment conditions; therefore, the solution obtained reflects the superposition principle. In addition, the obtained general solution to the boundary problem defines the distribution of steady temperature field in a multi-layered structure in the form of a prism with randomly arranged specialized tubular heaters of heat-generating modules of MEHHS.

---

### 5. Results of the study into formation of optimum temperature parameters of the microclimate at livestock facilities

---

The result of solving the problem on determining the influence of thermal conductivity of HS on the formation of temperature field in the multi-layered structure of a heating floor is the obtained functional dependence of temperature of the floor surface. Specifically, one of the components of the solution to a given problem takes into consideration effect of air environment heat over TAZ, a temperature of deep soil and soil behind the side wall of MEHHS, as well as the power consumed by each separate heating element of STH. Thus, we established the relationship between the

specified normative values of temperature for heating the surface of a floor and the power of energy fluxes, which are supplied to the heating elements of heat-generating modules of MEHHS, which makes it possible to implement structural-functional control over energy fluxes in HS. In addition, structural-functional control over energy fluxes in HS will ensure high efficiency and accuracy when maintaining the preset temperature modes of heating the floor surface in TAZ. This allows for efficient use of electricity generated by traditional and URSE sources, maximal accumulation of the “surplus”, operation under the mode “consumer–regulator”, ensuring quality of technological processes for producing livestock products under a mode of maximum energy saving. Computer computational experiments confirm that the proposed design of MEHHS could provide for the uniform heating of floor surface with an accuracy to 0.5 °C.

In this case, uniform heating of the floor surface at PF with a predetermined width can be achieved by a certain, for each of the modes (I–V), distribution of energy fluxes in MEHHS, that is, the level of capacity for heat release in specialized tubular heating elements in a two-dimensional system. The contribution of each heating element (heating pipe) of STH to the resultant thermal field on the surface of TAZ floor depends on its location in the HS assembly, heat exchange conditions on the boundary surfaces of heat-generating modules, and the power supplied to the heaters of STH.

Visualization of the process of MEHHS parameters optimization at different values of temperature on the floor surface is shown in Fig. 2, 3. Thus, Fig. 2, 3 show the expected distribution of temperature on the floor surface for the heating levels  $t_n=18\text{ °C}$  and  $t_n=38\text{ °C}$  for heating modes V, at different values of heat losses through a side wall of MEHHS: perfect heat insulation ( $a_s=0$ ), and  $a_s=0.75\text{ W/m}^2\cdot\text{K}$  and  $a_s=1.5\text{ W/m}^2\cdot\text{K}$ .

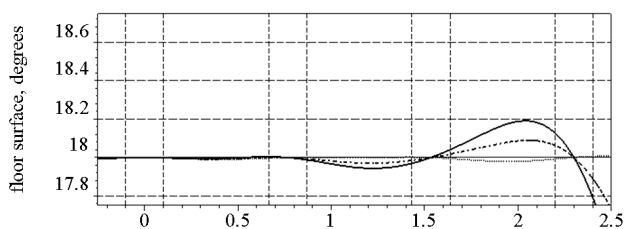


Fig. 2. Distribution of temperature at the floor surface at heat stabilization of HS for mode V at a temperature of 18 °C: 1 – capacity of heaters of the first tier; 2 – capacity of heaters of the second tier; 3 – capacity of heaters of the third tier

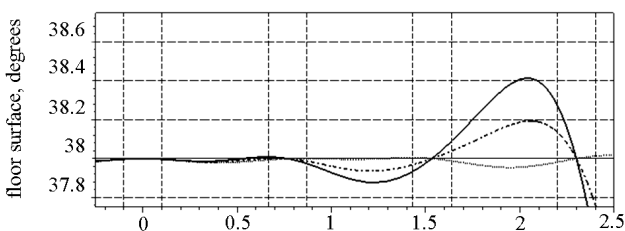


Fig. 3. Distribution of temperature at the floor surface at heat stabilization of HS for mode V at a temperature of 38 °C: 1 – capacity of heaters of the first tier; 2 – capacity of heaters of the second tier; 3 – capacity of heaters of the third tier

The power is supplied to the 1st, 2nd, or 3rd tiers, respectively; in this case, energy fluxes arrive to the heaters

of STH whose pipes are located along the width of the floor in the 8th, 6th, or 4th layers of MEHHS. In this case, defined by the mode, the 9th, 7th, or 5th STH are connected. Fig. 2, 3 exhibit, given the symmetry of the heating structure, only the right half of the heating floor of MEHHS ( $0 < y < 2.5i$ ), where we show at the corresponding points along the OY axis the energy charts of relative levels of linear power of STH. It is shown that the assigned level of heating of the floor surface is provided at the points of projections of STH axes onto the floor surface; we observe deviations from a given level among them; in this case, the deeper the active layer, the larger they are [4, 14]. Similar distributions of temperature fields for modes II and IV were also analyzed for various levels of heat losses at several variants of redistribution of energy fluxes between two active tiers of MEHHS. Fluctuations in temperature at the floor surface in this case also does not exceed 0.5–1 °C.

### 6. Discussion of results of the formation of temperature parameters of livestock facilities

By applying results of research into devised method for determining the impact of temperature field distribution inside the heating structure of MEHHS and scientifically substantiated structural parameters and controlled operation modes of heat-generating modules while strictly maintaining the preset values of temperature of the heating floor surface, it was possible to reduce energy intensity of technological processes for producing pork by 35–40 %. In addition, the use of the proposed MEHHS in the microclimate systems of livestock facilities, which operate in line with a bottom-up principle, while maintaining the preset values of temperature at the surface of a heating floor, makes it possible to reduce unit cost of feed stock by 8–10 %, to minimize the loss of young animals from colds and decrease the negative impact of waste generated by livestock production on the environment.

When designing multilevel electro heat accumulation systems, enabling thermal modes of microclimate at production livestock facilities in agriculture through the implementation of our solutions makes it possible to formulate proposals for further development of electrotechnical means for providing energy-efficient modes of MEHHS operation. This could be achieved by applying the structural-functional control over energy fluxes of power supply to STH heaters of heat-generating modules of MEHHS using the energy of traditional and URSE sources.

In comparison with existing systems for providing temperature regime of the microclimate of livestock facilities, development of electrotechnical systems that include the proposed multi-level heat-generating modules that enable strict control over preset temperature modes at the floor surface, makes it possible to ensure energy efficient formation of optimal temperature parameters of the microclimate while operating under the mode consumer–regulator. The results obtained are a continuation of earlier studies into MEHHS, which we plan to improve in the future.

### 7. Conclusions

1. We have obtained a general solution to the boundary value problem on determining the distribution of a steady temperature field in the multi-layered structure of MEHHS in the

form of a prism with randomly arranged tubular heat sources. The minimum temperature difference is in the range of 0.5–2 °C and is related to the temperature of air in the room of 8 °C. The maximum temperature difference is in the range of 1–4 °C and is related to the temperature of air in the room of 32 °C.

2. The mathematical model of MEHHS that we constructed solves the task on the optimization of formation of

temperature parameters of the heating floor surface with an accuracy to 0.5–1 °C. When supplying energy only to the bottom tier for the level of heating the floor of 38 °C, maximum temperature of the floor surface at a width of band of the heating floor of 1.8 m is 38.7 °C. The minimum floor surface temperature under a given mode is 37.8 °C at a width of band of the heating floor of 0.7 m.

## References

1. Romanchenko N. A. Analytical studies of the distribution of temperature field in the multilayer structure of the electrically heated floor // Herald of KhDTUSG them. P. Vasilenko «Problems of energy supply and energy saving in the agroindustrial complex of Ukraine». 2017. Issue 187. P. 84–87.
2. Review on thermal energy storage with phase change materials and applications / Sharma A., Tyagi V. V., Chen C. R., Buddhi D. // Renewable and Sustainable Energy Reviews. 2009. Vol. 13, Issue 2. P. 318–345. doi: 10.1016/j.rser.2007.10.005
3. Kuznik F., Virgone J. Experimental assessment of a phase change material for wall building use // Applied Energy. 2009. Vol. 86, Issue 10. P. 2038–2046. doi: 10.1016/j.apenergy.2009.01.004
4. Energy-saving electrotechnologies to ensure the standards of the thermal regimen of production facilities of agroindustrial complex with electric heating floors / Romanchenko N. A., Masorenko D. I., Slesarenko A. P., Soroka O. S. // Electrify and automated Agriculture. 2006. Issue 2. P. 82–92.
5. Effect of microclimate on the airborne dust and endotoxin concentration in a broiler house / Vučemilo M., Matković K., Vinković B., Macan J., Varnai V. M., Prester L. J. et. al. // J. Czech Anim. Sci. 2008. Vol. 53. P. 83–89.
6. Identification of the risk factors for high airborne particle concentrations in broiler buildings using statistical modelling / Banhazi T. M., Seedorf J., Laffrique M., Rutley D. L. // Biosystems Engineering. 2008. Vol. 101, Issue 1. P. 100–110. doi: 10.1016/j.biosystemseng.2008.06.007
7. Effect of microclimate on particulate matter, airborne bacteria, and odorous compounds in swine nursery houses / Yao H. Q., Choi H. L., Lee J. H., Suresh A., Zhu K. // Journal of Animal Science. 2010. Vol. 88, Issue 11. P. 3707–3714. doi: 10.2527/jas.2009-2399
8. Krommweh M. S., Rösmann P., Büscher W. Investigation of heating and cooling potential of a modular housing system for fattening pigs with integrated geothermal heat exchanger // Biosystems Engineering. 2014. Vol. 121. P. 118–129. doi: 10.1016/j.biosystemseng.2014.02.008
9. Li H., Rong L., Zhang G. Study on convective heat transfer from pig models by CFD in a virtual wind tunnel // Computers and Electronics in Agriculture. 2016. Vol. 123. P. 203–210. doi: 10.1016/j.compag.2016.02.027
10. Modelling heat and mass transfer of a broiler house using computational fluid dynamics / Rojano F., Bournet P.-E., Hassouna M., Robin P., Kacira M., Choi C. Y. // Biosystems Engineering. 2015. Vol. 136. P. 25–38. doi: 10.1016/j.biosystemseng.2015.05.004
11. Tabunshchikov Yu. K., Brodach M. Energy-efficient buildings. Moscow: ABOK-PRESS, 2003. 193 p.
12. Studentsov P. N. Warm floors in cattle-breeding premises. Moscow: Stroyizdat, 1989. 44 p.
13. Modelling of internal environmental conditions in a full-scale commercial pig house containing animals / Seo I., Lee I., Moon O., Hong S., Hwang H., Bitog J. P. et. al. // Biosystems Engineering. 2012. Vol. 111, Issue 1. P. 91–106. doi: 10.1016/j.biosystemseng.2011.10.012
14. Multilevel electrocontrol systems in the microclimate systems of the industrial complexes of the agroindustrial complex / Romanchenko N. A., Slesarenko A. P., Soroka O. S., Rumyantsev O. O. // Visnyk KhNTUSH im. P. Vasilenko «Improvement of technology and equipment for livestock production». 2005. Issue 42. P. 247–252.